

# Structured Chaos in a Devil's Staircase of the Josephson Junction

Yu. M. Shukrinov,<sup>1</sup> A. E. Botha,<sup>2</sup> S. Yu. Medvedeva,<sup>1,3</sup> M. R. Kolahchi,<sup>4</sup> and A. Irie<sup>5</sup>

<sup>1</sup>*BLTP, JINR, Dubna, Moscow Region, 141980, Russia*

<sup>2</sup>*Department of Physics, University of South Africa, P.O. Box 392, Pretoria 0003, South Africa*

<sup>3</sup>*Moscow Institute of Physics and Technology (State University), Dolgoprudny, Moscow Region, 141700, Russia*

<sup>4</sup>*Institute for Advanced Studies in Basic Sciences, P.O. Box 45195-1159, Zanjan, Iran*

<sup>5</sup>*Department of Electrical and Electronic Systems Engineering,  
Utsunomiya University, 7-1-2 Yoto, Utsunomiya 321-8585, Japan*

(Dated: December 5, 2021)

The phase dynamics of Josephson junctions under external electromagnetic radiation is studied through numerical simulations. Current-voltage characteristics, Lyapunov exponents and Poincaré sections are analyzed in detail. It is found that the subharmonic Shapiro steps at certain parameters are separated by structured chaotic windows. By performing a linear regression on the linear part of the data, a fractal dimension of  $D = 0.868$  is obtained, with an uncertainty of  $\pm 0.012$ . The chaotic regions exhibit scaling similarity and it is shown that the devil's staircase of the system can form a backbone that unifies and explains the highly correlated and structured chaotic behavior. These features suggest a system possessing multiple complete devil's staircases. The onset of chaos for subharmonic steps occurs through the Feigenbaum period doubling scenario. Universality in the sequence of periodic windows is also demonstrated. Finally the influence of the radiation and Josephson junction parameters on the structured chaos is investigated and it is concluded that the structured chaos is a stable formation over a wide range of parameter values.

PACS numbers: 05.45.-a, 82.40.Bj, 74.50.+r, 85.25.Cp

## I. INTRODUCTION

Nonlinear dynamical systems like the Josephson junction exhibit a wide variety of chaotic phenomena and are an interesting field of research for both the fundamental and applied sciences [1, 2]. Much progress has been made through numerical simulations of many important characteristics of chaos [3]. Investigations of critical exponents in various routes to chaos, such as period-doubling bifurcations, intermittency, and quasiperiodicity lend support to the universality and scaling behavior predicted by theoretical models [4]. In a Josephson junction driven by an external microwave radiation, the devil's staircase structure is realized as a consequence of the interplay of the Josephson plasma frequency, and the applied frequency (see Refs.[5, 6] and references therein).

The devil's staircase appears in other systems including the infinite spin chains with long-range interactions [7], frustrated quasi-two-dimensional spin-dimer system in magnetic fields [8], systems of strongly interacting Rydberg atoms [9], and in fractional quantum Hall effect [10]. The synchronization of Josephson and Bloch oscillations results in the quantization of transresistance which also leads to a devil's staircase structure.[11] Devil's staircase in a spin-torque nano-oscillator driven by a microwave field was experimentally demonstrated in Ref. [12].

In earlier studies of the rf-current-driven JJ it was found that, depending on the amplitude of the rf current, the system would develop a chaotic character [13–16]. It was also shown that the onset of chaos as a function of frequency correlated with the function that indicated infinite gain, also as a function of frequency, for the un-

biased parametric amplifier [17]. More recently the importance of chaos in intrinsic JJs, and its effects on the IV-characteristics and the Shapiro steps in these systems, were stressed in Refs. [18, 19].

In a further comprehensive study, the critical behavior of the dynamical equation, in the sense of how it goes from regular to chaotic, was investigated [20]. It was discovered that the critical behavior is that of the circle map. Here, in the subcritical state, the resonances are separated by quasi-periodic orbits (i.e. having irrational winding number), whereas in the supercritical state the dynamics is composed of chaotic jumps between resonances. The chaos appears to be the result of the resonance overlap [21]. In a similar study, the interaction of the Josephson junction with its surroundings was considered by coupling it in parallel with an RLC circuit, modeling a resonant cavity [22]. In this case the chaos develops through the familiar infinite sequence of period doubling bifurcations.

Other studies exist that try to understand the irregular response of dissipative systems driven by external sources when such behavior is interleaved by the synchronized motion (Shapiro steps). This so called intermittent chaos is modeled by a random walk between the two neighboring steps that have become unstable. A simple physical model was proposed in Ref. [23] and used for an analytic calculation of the power spectrum of the intermittent-type chaos occurring in rf- and dc-current-driven Josephson junctions. It was shown that the power spectrum of the voltage correlations has a broadband background characterizing the chaotic solution. A similar random walk model was developed to explain the phase synchronization of chaotic rotators [24].

The microwave-induced devil's staircase structure and chaotic behavior in current-fed Josephson junctions were studied experimentally and through analog simulations within the RCSJ model in Ref. [25]. Many externally driven dissipative systems demonstrate the occurrence of sequences of periodic states separated by gaps of a chaotic or intermittent nature.[23]. Different features and types of intermittent transitions to the chaotic state were investigated in Refs. [23, 26–29]. The RCSJ model was used to study the onset of chaotic behavior in the overdamped JJ, where a transition from unlocked quasiperiodic motion via subharmonic locked steps to the chaotic region occurs [5, 30]. In dynamical systems, intermittency is the temporal irregular alternation of phases between apparently periodic and chaotic dynamics. Pomeau and Manneville described three routes to intermittency when a nearly periodic system shows irregularly spaced bursts of chaos [31–33]. These, types I, II and III respectively, correspond to the approach to a saddle-node bifurcation, a subcritical Hopf bifurcation, and an inverse period-doubling bifurcation. Type III intermittency was also observed in Ref. [29]. In all the above mentioned types of intermittency the width of each phase is unpredictable.

We could also have other physical systems with competing frequencies leading to the devil's staircase structure. In a system with magnetic vortex oscillations, the sense of gyration of the magnetic vortex depends on the vortex core polarity, and can undergo sudden reversals as a critical velocity is reached. Driving currents can tune the self-sustained vortex oscillations and the frequency of the core reversals, resulting in phase-locked or chaotic states, within a devil's staircase structure [34]. In two capacitively coupled Josephson junctions, the phase-locked structure of the oscillations forms a devil's staircase, and chaotic dynamics develops between the main resonances as this coupling capacitance passes a critical value [35]. Another realizable model that goes chaotic via the resonance overlap in the devil's staircase structure, involves a modified Chua's circuit [36]. A class of models involve transport in an external potential; the resonance manifests itself in an enhanced diffusion constant [37]. Addition of competing forces, including noise, could result in anomalous transport and chaos; the predicted absolute negative mobility could be tested in a resistively and capacitively shunted Josephson junction [38]. The ensuing devil's staircase in the dynamics of a charged particle as it moves in electrostatic waves is a rare instance of a time dependent potential for which the effect has been observed [39].

In the present paper, we demonstrate a novel type of chaos, which for good reasons, is called structured chaos. The chaotic behavior we deal with here is set against the devil's staircase structure in the IV-characteristics of an underdamped Josephson junction at some parameters of the system, and in the presence of external radiation. The positions of the steps in the structure is determined by a continued fraction formula [40], so that the transformations of the regular behavior in the step's current

intervals to the chaotic ones is strongly synchronized. We show that in the chaotic windows we see remnants of this staircase, and we present more details of this structurally chaotic behavior. We discuss the role of the subharmonic subset of steps in the staircase, in bringing about such a structure, and discuss ideas having to do with the presence of multiple staircases [41].

The paper is organized as follows. In Sec. II we introduce the model and briefly describe the simulation procedure and parameters of the model and simulations. The IV-characteristics of the JJ under external radiation demonstrating structured chaos (alternating changes of the steps and chaotic regions, with changing bias current) are presented. We analyze the main features of this structure and calculate its fractal dimension. The chaotic nature of the IV-characteristic portions between steps is discussed based on high precision calculation of the Lyapunov exponents and the Poincaré section in Sec. III. In Sec. IV we discuss some unifying properties, particularly, the backbone features and Farey sum rule. The scaling features and on-step positive LE are analyzed in Sec. V. In Sec. VI we present the results of the influence of the radiation and JJ parameters on the structured chaos. Sec. VII is devoted to the analysis of the existing experimental results. Finally, Sec. VIII concludes the paper.

## II. SUBHARMONIC STEPS

First we discuss the features of the JJ IV-characteristics under external electromagnetic radiation. To simulate the IV-characteristics we use the resistively and capacitively shunted junction (RCSJ) model [42, 43] for the Josephson junction driven by both ac and dc current sources. This model is equivalent to that for a pendulum with dissipation, and driven by an external torque with both constant and periodic components. The model equations for the phase difference  $\varphi$  across the junction, taking into account the external radiation with frequency  $\omega$  and amplitude  $A$ , are

$$\dot{V} + \sin(\varphi) + \beta\dot{\varphi} = I + A\sin(\omega t), \quad (1)$$

$$\dot{\varphi} = V. \quad (2)$$

Here the dc-bias current  $I$  and ac amplitude  $A$  are normalized to the critical current  $I_c$ , the voltage  $V$  to  $V_0 = \hbar\omega_p/(2e)$ , where  $\omega_p$  is the plasma frequency, and time  $t$  to  $\omega_p^{-1}$ . The dissipation parameter is  $\beta = \beta_c^{-1/2}$ , where  $\beta_c$  is McCumber's parameter. Overdot indicates derivative with respect to the dimensionless time  $t$ .

To simulate the experimental conditions we have tested the effect of adding white noise to the bias current, with amplitude  $I_{\text{noise}} = 10^{-8}$ . The amplitude of the noise current was also normalized to the critical current  $I_c$ . We found that the features of IV-characteristics discussed in this paper do not depend on the noise in current, at this amplitude.

In the numerical simulations for this study we set  $\beta = 0.3$  (mostly), and  $I_{\text{noise}} = 0$ . We make use of a fourth-order Runge-Kutta integration scheme, using a time step of  $1/32$ , with  $10^4 - 10^5$  as a time domain for averaging,  $10^3 - 10^5$  units before averaging, and  $10^{-5} - 10^{-6}$  as the step in the bias current. Further details concerning the simulation procedure can be found in Refs. [44, 45].

The IV-characteristics of the JJ with dissipation parameter  $\beta < 1$  are given by the Stewart-McCumber model that predicts the hysteresis [42, 43]. The result of a simulation of IV-characteristics of a JJ at  $\beta = 0.3$ , and without radiation is presented in the inset to Fig. 1(a). The addition of external electromagnetic radiation, char-

disappears. The IV-characteristics of the JJ at  $\omega = 0.5$  and  $A = 0.8$  is shown in the main part of Fig. 1(a). We see that there is no hysteresis in comparison with the case at  $A = 0$  or small  $A$  (see Ref. [40]) and chaos develops within some current intervals. Figure 1(a) indicates that the model has the propensity for both resonance and chaos. For analysis of the observed Shapiro steps and their subharmonics, we use an algorithm proposed in Ref. [40]. According to it the steps in the staircase structures form continued fractions with voltages determined by

$$V = \left( N \pm \frac{1}{n \pm \frac{1}{m \pm \frac{1}{p \pm \dots}}} \right) \omega, \quad (3)$$

where  $N, n, m, p, \dots$  are positive integers. Truncating Eq. (3) at  $N$  gives the first-level terms of the continued fraction, corresponding to the main Shapiro step, or harmonics. Similarly, truncating the formula at  $n$  gives the second-level terms, corresponding to subharmonic Shapiro steps, etc.

There is a manifestation of a Shapiro step at  $V = \omega = 0.5$  and its harmonics at  $V = 1, 1.5, 2, 2.5, 3$ , as shown in Fig. 1(a) by arrows below the corresponding numbers. In the chaotic region we observe transitions between states related to the different SS harmonics, as the current varies. In particular, very intensive transitions occur between the second, third and fourth SS harmonics. The IV-curves in Fig. 1 were obtained by sweeping the bias current from  $I = 0$  to  $I = 1.2$  and back to zero. Both curves (obtained by going up and down in current) coincide, showing no hysteresis.

In this paper we concentrate on that part of the IV-characteristic marked by circle in Fig. 1(a). An enlarged view of the encircled region is shown in Fig. 1(b), where a series of steps, in the form of  $(N - (1/n))\omega$ , is observed between  $\omega$  and  $2\omega$ , i.e. for  $N = 2$  and  $n$  a positive integer. We note that these steps approach the second Shapiro step from below. An interesting feature of this staircase is the structured chaos (alternating changes of the steps and chaotic regions, with changing bias current) that materializes along with it; i.e., we have alternating windows of resonance and chaos. We name this structure “Svetlana” [46]. The manifestation of such type of structures are present in the numerical simulations of other authors as well, although it has not been identified explicitly before. Particularly, in the structure between the forth and fifth SS, shown in the inset to Fig.13 of Ref. [47], we can see the subharmonic steps separated by chaotic parts. But in the present case the Svetlana structure represents the complete structure between two SS (i.e. between  $V = 0.5$  and  $V = 1$ ). The steps appear at voltages  $\omega, 3\omega/2, 5\omega/3, 7\omega/4$ , etc., and approach the second SS harmonic at  $V = 1$ . The regular step width (SW) and chaotic part width (CPW) of the subharmonics in Svetlana are presented in Fig. 2(a). We see that starting from the step  $5/3$  the width of the chaotic part to

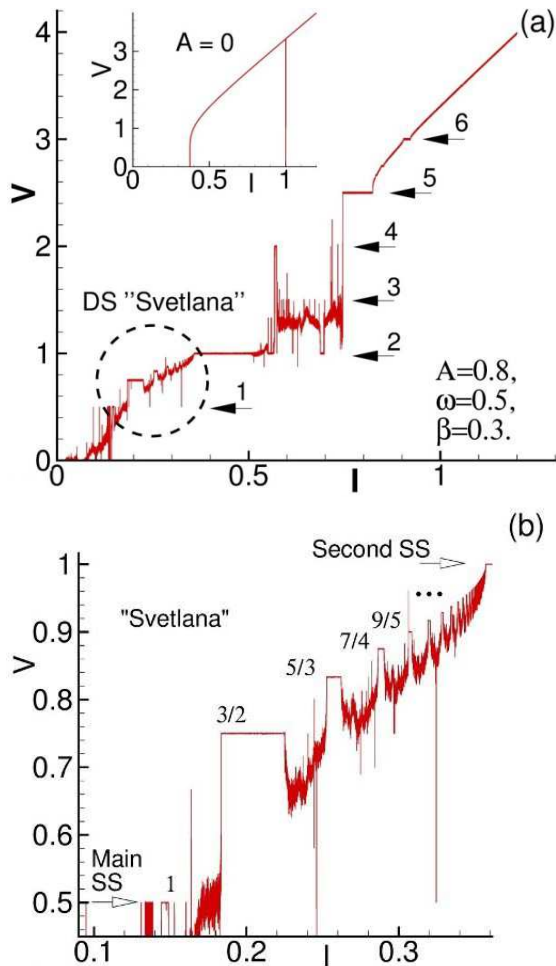


FIG. 1: (Color online) (a) The IV-characteristics of the JJ at  $\beta = 0.3$ ,  $\omega = 0.5$  and  $A = 0.8$ . Arrows with numbers indicate SS harmonics. The inset shows the IV-characteristic without radiation; (b) The enlarged part of the IV-characteristics (“Svetlana”) marked by the circle in (a), demonstrating the steps alternating with chaotic regions. These subharmonic steps are numbered according to the second level of of the continued fraction formula  $V = (2 - (1/n))\omega$ , with  $n = 1, 2, \dots$

acterized by the additional current  $A \sin(\omega t)$  in Eq. (1), leads to the appearance of Shapiro steps and their subharmonics. At high amplitude of radiation the hysteresis

the right of each step becomes larger relative to the step width, while both parts decrease monotonically. The total width (TW), i.e.  $SW + CPW$ , is also shown in the figure, in this case by the square markers.

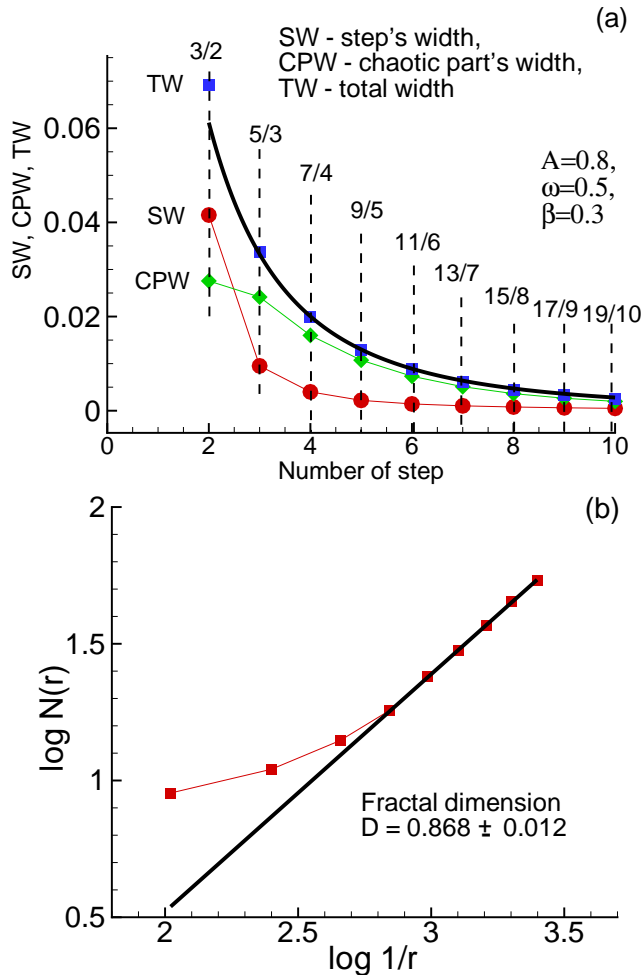


FIG. 2: (Color online) (a) The width of the steps (SW, circles), chaotic part widths (CPW, diamonds) and total width (TW, squares) for the Svetlana. The total width is the sum of SW and CPW. The solid black line is fitted from a Bohr, hydrogen-atom-type equation; (b) Determination of the fractal dimension  $D$  and its uncertainty via the box counting method [48]. See main text for details.

In view of the chaos that appears in the Svetlana, it is interesting to ask whether or not the structure is still complete, as in the case of the devil's staircase. In mathematical terminology the staircase is complete if the set not covered by the steps is of measure zero. For the complete devil's staircase this corresponds to a universal fractal dimension of close to 0.87 [5]. To estimate the fractal dimension of the Svetlana we followed the method described in Ref. [48]. Our results are summarized in Fig. 2(b), where we have determined the dimension  $D$  from the slope, as  $r \rightarrow 0$ , of a log-log graph of  $N(r)$  against  $1/r$ . Here  $N(r)$  is the minimum number of boxes

of dimension  $r$  required to contain all the points in the geometric object. As can be seen in Fig. 2(b), the number of boxes increases as the box size reduces, and in the limit as  $r$  becomes smaller the slope of the graph becomes constant. By performing a linear regression on the linear part of the data plotted in Fig. 2(b), i.e. using only the six points to the right of the figure, we obtained a dimension of  $D = 0.868$ , to within an uncertainty of  $\pm 0.012$ .

An interesting phenomenological feature that can be used to quantify the results in Fig. 1(b) is the trend that we observe in the width of the steps and the chaotic intervals interleaving them. We find that an equation of the same form as that of the Bohr atom, given by

$$l = l_0 \left( 1/n^2 - 1/(n+1)^2 \right), \quad (4)$$

describes the widths of the aforementioned intervals well. In this equation  $l_0$  is constant for the whole set of steps, and  $n$  is particular to a step. As we ascend the staircase, we go to higher  $n$ , consecutively. We find that the formula works to a high accuracy, irrespective of whether we only take the width of the steps, or we include the width of the chaotic windows, as if the staircase were intact. The thick line in Fig. 2(a) is a fit of Eq. (4) to the simulation data. The curious fact that the data is fit so well by Eq. (4) may be understood if we view the Bohr equation as a Padé approximant of an inverse cubic polynomial. Thus it has nothing to do with quantum mechanics. Such a fitting formula is nevertheless important for the present work because it determines the scaling properties of our results.

### III. STRUCTURED CHAOS

Portions of the IV-characteristics between neighboring steps in Fig. 1(b) result from chaotic dynamics. Such chaotic nature is confirmed by the calculation of the Lyapunov exponents (LE) and Poincare section (PS). Figure 3(a) shows the two non-trivial LEs (thinner red and blue lines) and IV-characteristic (thicker black line) as functions of the dc-bias current. The two LE obey the sum rule [15]  $\lambda_1 + \lambda_2 = -\beta$  and are therefore mirror images of each other with respect to the horizontal line at  $-0.15$  on the left hand scale. We see that the steps in the IV-characteristic coincide with regular behavior, as indicated by the negative regions of the maximal LE (shown in red online). On the other hand, in between steps we see that the maximal LE is positive, indicating chaotic behavior.

We note that PS analysis gives an effective method to investigate the Shapiro step subharmonics in the devil's staircase, as well as the chaotic dynamics. In Fig. 3 this is complemented by calculation of the LEs, indicating the position of bifurcations (when they touch zero) and chaos (when they go positive). The PS provide a vivid expression of synchronization between the Josephson frequency and the external drive, especially for the subharmonics.



In Fig. 3(b) we show the PS corresponding to the same structure as in (a). Here the section has been made by plotting the instantaneous steady state voltage, for each bias current, at precisely the times when the magnitude of the (sinusoidal) external radiation changes from negative to positive. We note that in the regular on-step regions these voltage values coincide and form continuous curves with respect to the changing bias current.

The number of PS curves within the regular regions, i.e. corresponding to the steps in the IV-characteristic, coincide with the denominator of the related term in the continued fraction sequence. This feature reflects the origin of the subharmonics which appear at voltage steps given by  $\omega_J = p\omega/q$ , where  $p$  and  $q$  are positive integers. These steps occur when the Josephson frequency is such that  $p$  cycles of the phase correspond precisely to  $q$  cycles of the external radiation. For example, the step at  $V = 5\omega/3$  corresponds to the  $3\omega_J = 5\omega$ .

Looking more closely at the bifurcation diagram we see that an increase of the bias current along any particular step causes a series of period doubling bifurcations which do not alter the constant value of the average voltage on the step. Such on-step period doubling bifurcations have been discussed in Ref. [3], for example.

#### IV. BACKBONE FEATURES AND FAREY SUM RULE

The distinguishing feature of the Svetlana is structured chaos. By structured chaos, we mean that the Svetlana can be understood as a set of steps belonging to a devil's staircase, that has been destroyed in a systematic way, so as to preserve the scaling properties of the original staircase. Here, we present heuristic arguments for this assertion, based on the results shown in Fig. 2–Fig. 5.

The scaling shared by the various sections of the steps, even the irregular parts, is shown in Fig. 2(a). The fractal property of the staircase is shown in Fig. 2(b). The latter property is a result of the synchronization between the Josephson frequency and the external radiation frequency, and it has been shown that the resulting structure seen in the Shapiro steps can be accurately reproduced by a continued fraction formula [40]. The different levels of this continued fraction form a self-similar structure, called the devil's staircase [49]. In this sense, Svetlana is what is left of a staircase that was to form a devil's staircase, and yet Svetlana keeps the scaling even in the irregular windows, again as seen in Fig. 2. This hints at an underlying structure that these apparently irregular regions have in common. Fig. 3 shows that these irregular variations of voltage with current refer to the chaotic dynamics of the system. We should note that the chaotic windows do not show monotonic variations of average voltage with current. This is in contrast to the structure of a complete devil's staircase; we will return to this aspect of Svetlana.

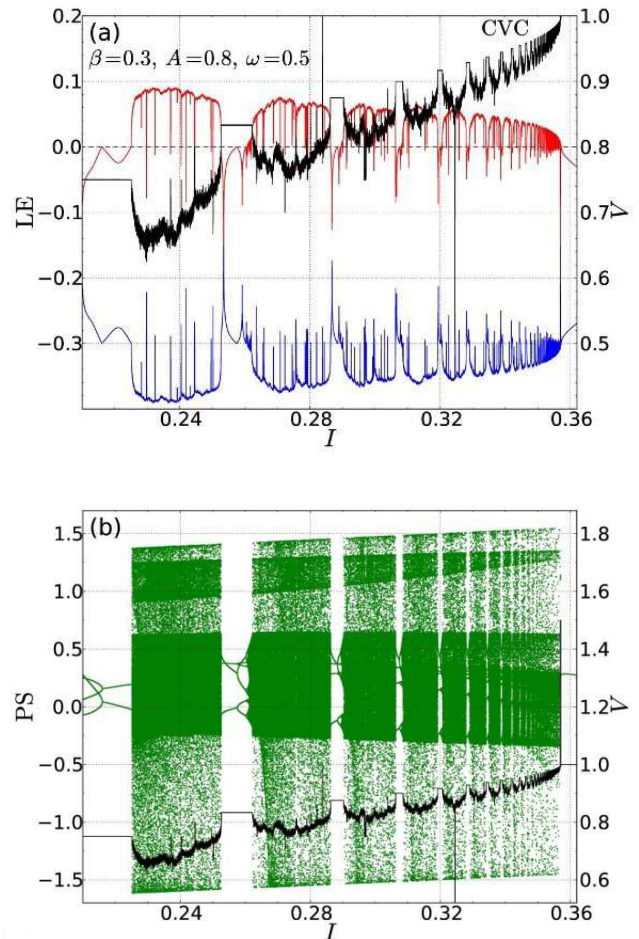


FIG. 3: (Color online) High precision calculation of (a) the Lyapunov exponents and IV-characteristic and (b) the Poincaré section and IV-characteristic (repeated for clarity) of the Svetlana structure.

According to Fig. 2 and Eq. (4), scaling in current can provide insight into the behavior of the junction, even when comparing the chaotic regions. We can map the chaotic windows onto each other using a linear mapping. For the purposes of the following analysis, we consider the first five chaotic windows that interleave the six steps:  $3/2$  (for  $n = 2$ ),  $5/3$  (for  $n = 3$ ),  $7/4$  (for  $n = 4$ ),  $9/5$  (for  $n = 5$ ),  $11/6$  (for  $n = 6$ ),  $13/7$  (for  $n = 7$ ). For simplicity we will refer to these windows as 1 through 5. We can define a correlation function as usual; i.e. by averaging over the product of voltages at corresponding times, at a given current, and normalizing to the self-correlated values. We have,

$$C(V_{I_{i\alpha}}, V_{I_{j\alpha}}) = \frac{\int_0^T V_{I_{i\alpha}}(t) V_{I_{j\alpha}}(t) dt}{\sqrt{(\int_0^T V_{I_{i\alpha}}^2(t) dt)(\int_0^T V_{I_{j\alpha}}^2(t) dt)}}. \quad (5)$$

Here,  $I_{i\alpha}$  denotes a specific current within the  $i$ th chaotic region ( $i = 1, 2, 3, 4, 5$ ), in which each region has been di-

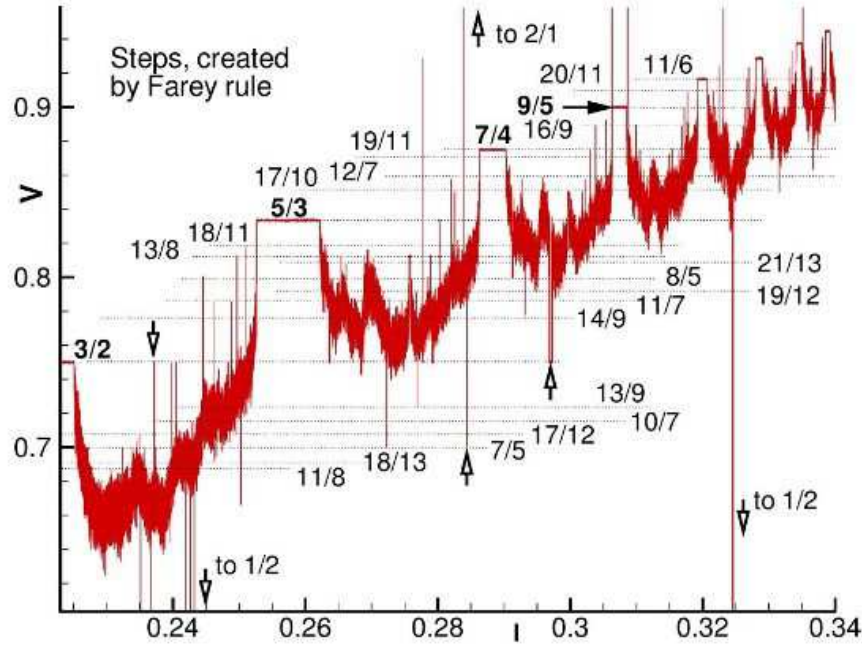


FIG. 4: (Color online) The underlying structure of the  $IV$  staircase as characterized by the Farey steps, even as part of the staircase has been destroyed by chaos. As an example, the Farey sequence  $3/2, 11/7, 8/5, 13/8, 5/3$ , is based on the Svetlana steps  $3/2$  and  $5/3$ .

vided into  $N$  equal current steps, i.e.  $\alpha = 1, 2, \dots, N$ . Equivalent currents are then defined by the linear relationship  $I_{i\alpha} = a_j (I_{j\alpha} - I_{j0}) + I_{i0}$ , where the  $a_j = (I_{iN} - I_{i0}) / (I_{jN} - I_{j0})$  are scaling factors. In this work we chose  $N = 550$  and made use of Simpson's  $3/8$  rule to evaluate the integrals over a time domain of  $T = 2000$  dimensionless units. We note that in calculating the correlation integrals, it is important to ensure that the phase of the driving force, i.e. the  $\sin(\omega t)$  term in Eq. (1), is the same at the start of the integration ( $t = 0$ ) for both signals  $V_{I_{i\alpha}}(t)$  and  $V_{I_{j\alpha}}(t)$ . If this is not the case, the correlations  $C(V_{I_{i\alpha}}, V_{I_{j\alpha}})$  are practically zero, as one might expect.

To bring out the scaling property of the step, specially the chaotic region that is now making up a part of it, as Fig. 2(a) is also showing, we compare the mentioned chaotic windows 1 through 5, in Fig. 5. As just mentioned, the current axis is scaled so that the chaotic regions for steps 1 through 5 span the same current interval (in length) as step 1 does. In Fig. 5(a) we have four of the voltage pair correlation functions, using Eq. (5) for these five chaotic regions. Fig. 5(b) shows the voltages for the five chaotic regions on this scaled axis, and Fig. 5(c) shows the Lyapunov exponents.

A closer look at Fig. 1(b) with the aim of revealing its fine structure is given by Fig. 4. The widest phase-locked region; i.e. the widest step, between any two resonances  $p/q$  and  $P/Q$  is known to be given by  $(p + P)/(q + Q)$  known as the Farey sum of the two rational numbers [48]. The Farey sum resonance is included in the continued

fraction, but at a level further down. The Svetlana steps are used to obtain the Farey steps; e.g. the sequence  $5/3, 17/10, 12/7, 19/11, 7/4$ , is based on  $5/3$  and  $7/4$ . We have shown the position of the Farey steps on top of the Svetlana, to emphasize the underlying structure in the blurred and chaotic regions.

In order to unify and explain these results, we highlight the presence of a multiple devil's staircase, associated with each step [41]. The results point to the equivalence of our model at the specified parameters, to a discrete map with two discontinuities. The usual devil's staircase is a monotonically increasing function, as manifested in the circle map. When discontinuities are introduced, this monotonicity is lost, and the phase-locked regions compose tower-like structures. That is, each step forms a mesa, associated with two devil's staircases, one ascending and leading to it; the other descending from it, until it joins the ascending staircase leading to the next plateau, given by the next step. This non-monotonic behavior in voltage as a function of current, as well as the formation of steps as mesas is clearly shown in Fig. 4. Another interesting feature of this figure is the brief presence of the various steps, as emphasized by the Farey steps. This is also confirmed by the negative Lyapunov exponents that signal remnants of the staircase. Based on these observations we conjecture that each chaotic interval is the result of resonance overlap in this backbone structure. The idea is that the chaos is the result of the deterministically chaotic wandering of the dynamics amongst the resulting Farey resonances, as they start to overlap. This

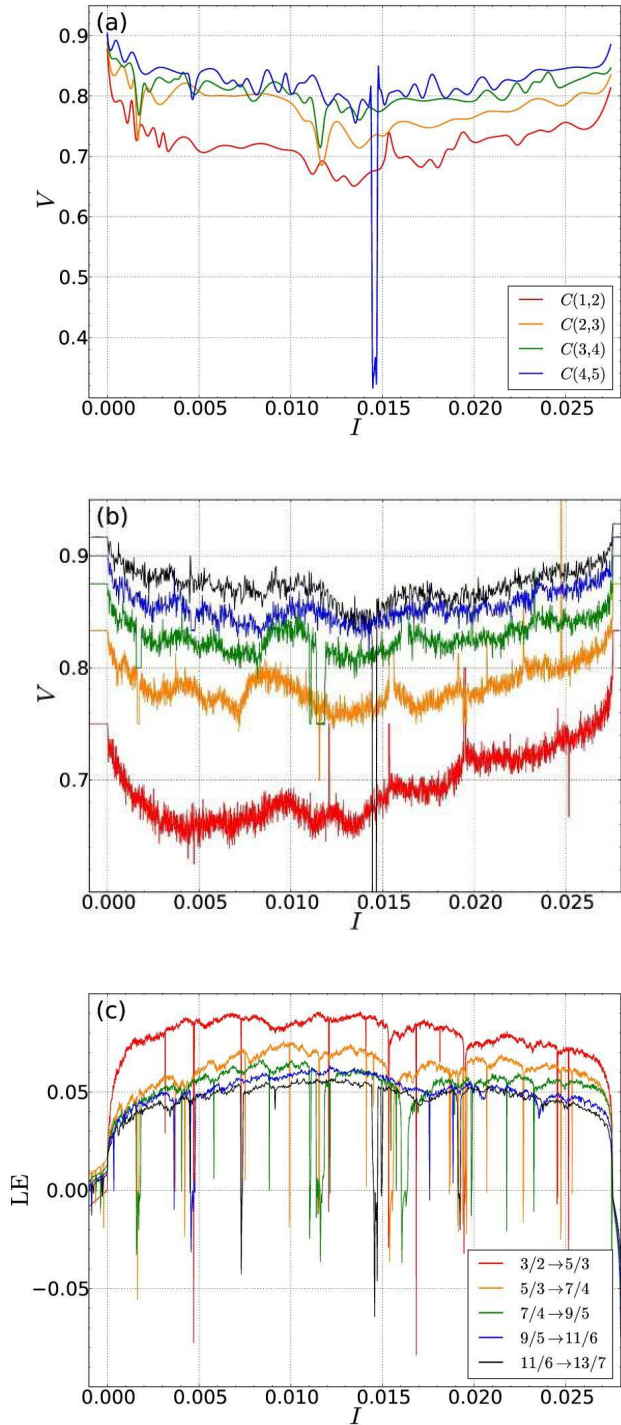


FIG. 5: (Color online) The scaling that brings structure to the chaotic windows. This is manifested in (a) that shows the pair correlations (1,2), (2,3), (3,4), (4,5), each between the consecutive chaotic windows. Another measure for this correlation is given in (b), where the average voltage is given on the scaled current axis; (c) The Lyapunov exponent for the dynamics at the scaled current.

is the main argument leading to what we have termed as structured chaos in the devil's staircase.

## V. CHAOS ON THE SUBHARMONIC STEPS OF THE SVETLANA

Although it has previously been shown that the onset of chaos, on certain *harmonic* steps of a single rf-biased junction, occurs through the Feigenbaum scenario [50, 51], the onset of chaos on *subharmonic* steps such as those occurring in the Svetlana has not been investigated previously. In the present section we will make use of extremely high-resolution simulation data to demonstrate that the route to chaos on the subharmonic steps of the Svetlana also occurs via the famous Feigenbaum scenario. Furthermore, our simulations reveal another interesting property of the Svetlana; namely, that the subharmonic steps are not immediately destroyed as the chaos sets in. We discuss this phenomenon in subsection C.

### A. Demonstration of Feigenbaum period doubling scenario

In the rf-biased Josephson junction, the Feigenbaum scenario was first identified by Huberman *et al.* [13] and later examined by many authors. (See, for example, Sec. 5.6 of Ref. [3] and the references therein.)

In Fig. 6 we show the behavior of the maximal LE and PS within a current interval corresponding to the transition from one of the subharmonic steps in the Svetlana to the chaotic region just to the right of the same step.

In this case we are considering the  $5\omega/3$  step that was previously shown in Figs. 1(b) and 3. As the edge of the step is approached with increasing bias current, the transition to chaos occurs via a sequence of period-doubling bifurcations. This sequence of bifurcations is infinite and, as we will show below, it follows Feigenbaum's the well-known universal scaling laws.

To test the scaling properties for the aforementioned bifurcation sequence we make use of the high-resolution simulation data that is plotted in Fig. 6. For this simulation we used a smaller than usual current step ( $\Delta I = 10^{-8}$ ) to locate the first seven values of the currents  $I_n$  at which the successive period-doubling bifurcation occur. The seven values so-obtained, including the value of current at the onset of chaos  $I_\infty$ , are listed in Table I. The values for  $I_n$  listed in Table I, produce successive approximations that converge to Feigenbaum's delta, which is defined as

$$\delta = \lim_{n \rightarrow \infty} \frac{I_n - I_{n-1}}{I_{n+1} - I_n}. \quad (6)$$

These successive approximations are listed in the third column of Table I. The best approximation found is  $\delta_6 = 4.6713$ , which is very close to the theoretical value of  $\delta = 4.6692$ .



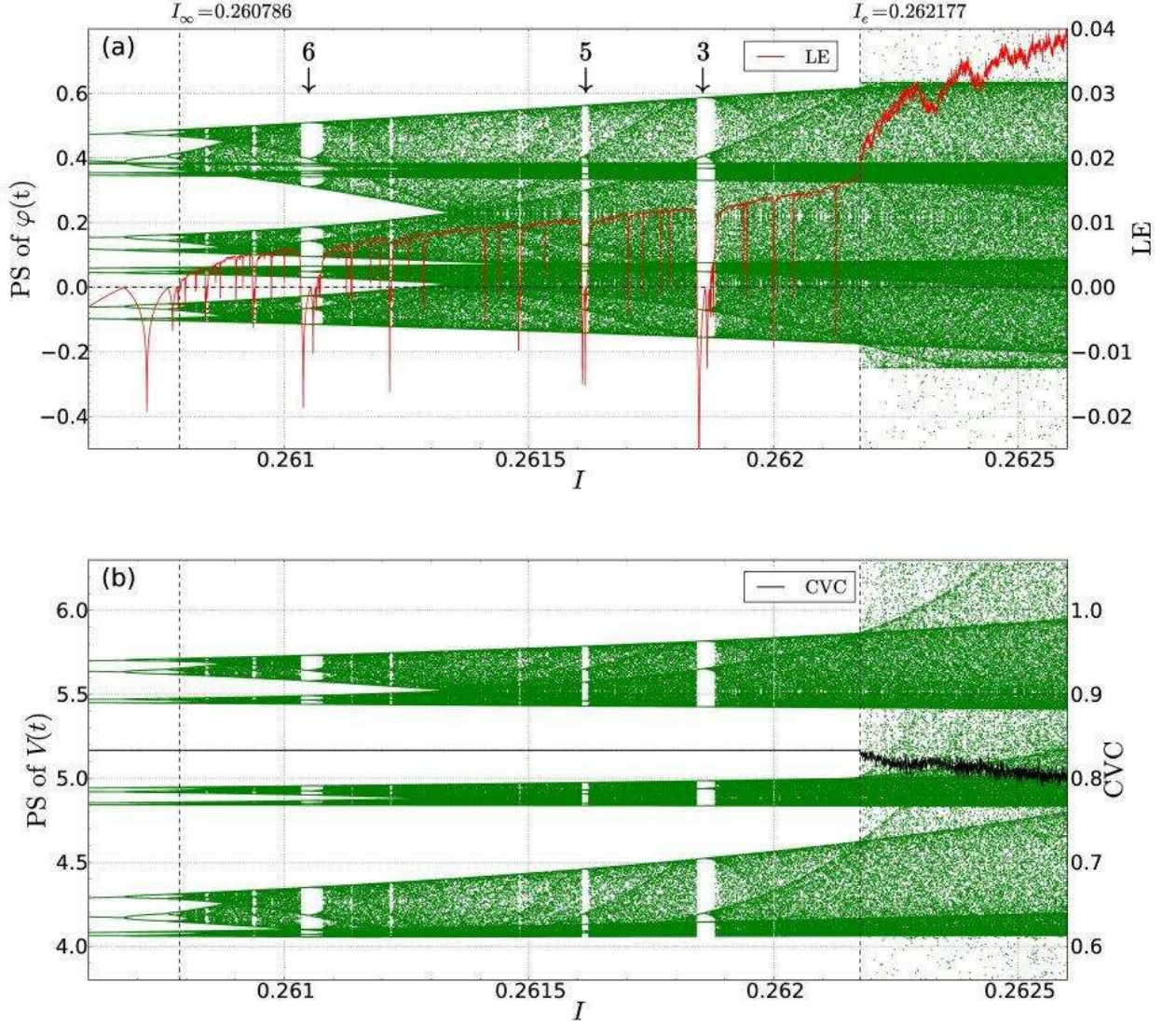


FIG. 6: (Color online) (a) Maximal Lyapunov exponent (solid red line) and Poincaré section of the phase (green dots) for bias currents corresponding to the right edge of the  $5\omega/3$  step; (b) Poincaré section of the voltage (green dots) and the average voltage (solid black line) over the same bias current range. In both figures the section plane for the PS coincides with times when the sinusoidal rf-bias signal crosses from negative to positive.

By measuring the maximal voltage differences  $d_n$ , separating the bifurcated branches shown in the PS, we also obtained three increasingly accurate estimates of Feigenbaum's scaling parameter  $\alpha$ , defined as

$$\alpha = \lim_{n \rightarrow \infty} \frac{d_n}{d_{n+1}}. \quad (7)$$

Successive values of  $d_n$  were determined to 5 decimal places, as listed in the fourth column of Table I. At this level of uncertainty the values of  $\alpha_n$  could be determined accurately up to  $n = 3$ , and the estimate so obtained is  $\alpha_3 = 2.503$ , which is also very close to the universal value of  $\alpha = 2.5029$ . Thus we have verified that the onset of chaos on the subharmonic steps of the Svetlana occurs

through Feigenbaum's famous period-doubling scenario.

### B. Universality in the sequence of periodic windows

Together with the aforementioned scaling laws for  $\delta$  and  $\alpha$ , another universal feature of the period doubling route to chaos is the sequence of periodic windows that occurs once the chaos has set in. In Fig. 6, and in Table I, we see that the accumulation point for the bias currents in period doubling sequence occurs at  $I_\infty = 0.260786$ . For currents higher than  $I_\infty$  the system is chaotic, except within a finite number of so-called periodic windows,



TABLE I: Calculation of the Feigenbaum numbers  $\alpha$  and  $\delta$  for the onset of chaos on the  $5\omega/3$  subharmonic step of the Josephson junction. Entries with three asterisks (\*\*\*) could not be determined from the simulation data to the same uncertainty as the listed entries.

$n$	$I_n$	$\delta_n = \frac{I_n - I_{n-1}}{I_{n+1} - I_n}$	$d_n$	$\alpha_n = \frac{d_n}{d_{n+1}}$
1	0.25756981	***	0.20707	2.956
2	0.26025001	6.3363	0.07004	2.505
3	0.26067300	4.7500	0.02796	2.503
4	0.26076205	4.6943	0.01117	***
5	0.26078102	4.6840	***	***
6	0.26078507	4.6713	***	***
7	0.26078594	***	***	***
$\vdots$	$\vdots$	$\vdots$	$\vdots$	$\vdots$
$\infty$	0.26078606	***	***	***

which can be observed clearly in both the PS, and the LE (the maximal LE becomes negative within each periodic window). We have found it convenient and more accurate to locate the periodic windows by looking for the regions over which the maximal LE drops below zero. In the present case, this method has enabled us to locate all the periodic windows wider than  $10^{-6}$  bias current units. For each window, listed in the order of increasing bias current, Table II shows the value of the bias current at the start (column 2) and end (column 3) of the window, together with the associated period  $T$  (column 4). Note that, because there are at least three branches in the PS for currents corresponding to the regular part of this  $5\omega/3$  step (c.f. Figs. 3 and 6(a)) we have normalized  $T$  to three times the external radiation period  $\tau = 2\pi/\omega$ .

TABLE II: The sequence of periodic windows occurring in the chaotic region shown in Fig. 6.

	$I_{\text{start}}$	$I_{\text{end}}$	$T/(3\tau)$
1	0.260797	0.260799	24
2	0.260838	0.260841	12
3	0.260936	0.260938	10
4	0.261033	0.261054	6
5	0.261136	0.261138	10
6	0.261215	0.261217	8
7	0.261479	0.261481	7
8	0.261608	0.261614	5
9	0.261843	0.261860	3

With this normalization the sequence of the larger periodic windows is 6, 5 and 3, as marked by the downward pointing arrows in Fig. 6(a), in the order of increasing bias current. This sequence has also been reported in Refs. [48, 52], albeit at different parameter values. Because this sequence of the main periodic windows has also been observed experimentally in a wide variety of other,

quite different dynamical systems, it has become known as a universal sequence (U-sequence). Note that in Table I we have not listed the periods of the period-doubling cascades which break up the larger periodic windows that have been marked in Fig. 6(a). However, closer examination of these windows reveals that their breakup also occurs through an infinite sequence of period doubling bifurcations, which is self-similar to the original sequence described above, in the sense that it not only obeys the Feigenbaum scaling laws, but again contains the universal sequence (6, 5 and 3 etc.) of periodic windows at a much finer scale. These tiny periodic windows are of course virtually impossible to observe experimentally. Our simulation data, however, clearly predicts that the chaos observed on the subharmonic steps of the Svetlana, also contains a U-sequence of stable periodic orbits.

### C. On-step positive Lyapunov exponent

An interesting feature of the chaotic region shown between  $I_\infty$  and  $I_e$  in Fig. 6, is the on-step positive Lyapunov exponent. By this we are referring to the fact that the average voltage throughout this range of bias current remains constant, even though the LE becomes positive, i.e. the system becomes chaotic. This type of behavior has also been observed in the numerical simulations of Kautz [3], where it was reported for a transition to chaos that occurs on a harmonic step. In the present case we observe the same behavior on a subharmonic.

The persistence of the average voltage step, even when the system trajectory becomes chaotic, can be understood by looking at the PS of the initial phases shown in Fig. 6(a). Between  $I_\infty$  and  $I_e$  it is clear that the initial phases remain range bound, approximately between  $-0.19$  and  $0.61$ . On the other hand, for bias currents larger than and  $I_e$  the phases span the full range  $(-\pi, \pi]$ . For this reason, the chaos that occurs between  $I_\infty$  and  $I_e$  was referred to by Kautz [3] as phase-locked chaos. However, unlike the case of an harmonic step, where the phase always advances by approximately  $2\pi$  on every rf-cycle; in the present case the rf-amplitude is sufficiently large to cause reversals, so that in the present case the phases may either advance or reduce by approximately  $2\pi$  on every rf-cycle. If one interprets this behavior in terms of a particle on a washboard potential, then the particle is able to advance or retreat by one or two wells on any given rf-cycle, which means that it is diffusive in nature, in spite of being phase-locked. (Note that, as defined by Kautz, the term phased-locked refers to the fact that phase is highly correlated (but not strictly-speaking locked) to the rf-cycle.) Thus, the distinction made between phase-locked and diffusive chaos in Ref. [3], breaks down in the present case and more work would be required to investigate the transition that occurs here, in going from the phased locked region between  $I_\infty$  and  $I_e$ , to the diffusive region, for currents above  $I_e$ . For the case of an harmonic step without reversals, the transition oc-

curred via a chaotic crisis.[3]

In the present article we will not investigate the nature of this transition in greater detail. It suffices to note that, as the current is increased beyond  $I_e = 0.262177$ , the  $5\omega/3$  step breaks up as the average voltage becomes erratic. It can be seen in Fig. 6(a), that the disintegration of the step is accompanied by a sharp increase in the already positive LE.

## VI. DEPENDENCE OF SVETLANA ON RADIATION AND JJ PARAMETERS

At a fixed frequency  $\omega = 0.5$  and dissipation parameter  $\beta = 0.3$  the most pronounced structured chaotic formation (Svetlana) is observed around  $A = 0.8$ . A natural question appears: can changes of JJ or radiation parameters lead to a devil's staircase structure without chaotic windows? That is, does Svetlana appear as an intermediate structure of synchronized steps before transition to chaos, or does what we have come to term structured chaos "possess equal rights" in JJ dynamics under radiation, as for other types of devil's staircase formations?

To answer this question we discuss here the variation of the Svetlana with changes in the amplitude of radiation. The structures at three values of the amplitude,  $A = 0.75, 0.8, 0.85$  are presented in Fig. 7. As we have seen in Fig. 1(b), the main SS harmonics at  $V = 0.5$  is not stable at the chosen JJ and radiation parameters, so we analyze the features between the subharmonic  $3\omega/2$  and the second SS at  $V = 2\omega$ . The known fact is that, with an increase in amplitude of external radiation, the width of Shapiro harmonics changes, following the Bessel function dependence [1, 53]. Analysis shows (and it is clear from Fig. 7) that with an increase in  $A$  the position of the onset of the second SS harmonic at  $V = 2\omega$  is shifting more in comparison to the shifting of the first SS harmonic at  $V = \omega$ . That is, the current interval between the beginning of the second SS harmonics and the end of the first one is reduced at  $A = 0.8$  in comparison to  $A = 0.75$  and increased in comparison to  $A = 0.85$ . These changes are consistent with the expected Bessel function dependence.

First, we consider the effect of decreasing the radiation amplitude by comparing the two structures at  $A = 0.75$  and  $A = 0.80$ , as shown in Figs. 7(a) and (b). We see that the decrease in  $A$ , from  $A = 0.80$  to  $A = 0.75$ , shifts the devil's staircase structure to the right side of the considered current interval. The overall structure is stretched, while the widths of the steps are decreased, i.e. the widths of the chaotic windows increased as  $A$  decreased from  $A = 0.80$  to  $A = 0.75$ . This trend continues with a further decrease in the amplitude of radiation (not shown here), eventually leading to the disappearance of the Svetlana structure. Thus we do not observe the structure without chaotic windows. As  $A$  is reduced, we note the appearance of an additional step between  $5\omega/3$  and  $7\omega/4$ , marked by a circle in Fig. 7(a). This

additional step belongs to the third continued fraction level, determined by  $V = \left(N \pm \frac{1}{n \pm \frac{1}{m}}\right) \omega$  with  $N = 2$ ,  $n = 3$ , and  $m = 3$ . It is the  $13\omega/8$  step, with the corresponding value of voltage being 0.8125. This finding is in agreement with our hypothesis about the role of the backbone in the Svetlana (see Chapter IV).

Second, we consider the effect of increasing the amplitude of radiation by comparing the structures at  $A = 0.8$  and  $A = 0.85$  as presented in Fig. 7(b,c). There is a shift of the devil's staircase structure to the left side of considered current interval, and then there is a decrease in the width of the SS subharmonics. The current interval between the beginning of the second SS harmonics and the end of the first one is reduced at  $A = 0.85$  in comparison to  $A = 0.8$ . This shrinking of the devil's staircase structure has the same explanation as the stretching at  $A = 0.75$ . We note also the appearance of the  $3\omega/2$ -subharmonics in the current interval between  $5\omega/3$  and  $7\omega/4$  subharmonics in Fig. 7(c) and the appearance of the  $5\omega/3$  subharmonics in the current interval between  $7\omega/4$  and  $9\omega/5$  subharmonics. The corresponding part of IV-characteristic is enlarged in Fig. 7(d). These facts demonstrate an overlapping mechanism of the transition of synchronized steps to the chaotic state. With further increase in  $A$  the chaotic regions are expanded and devil's staircase structure disappears. So, an increase in the amplitude of radiation leads to a decrease in the subharmonic widths and a relative increase in the chaotic regions.

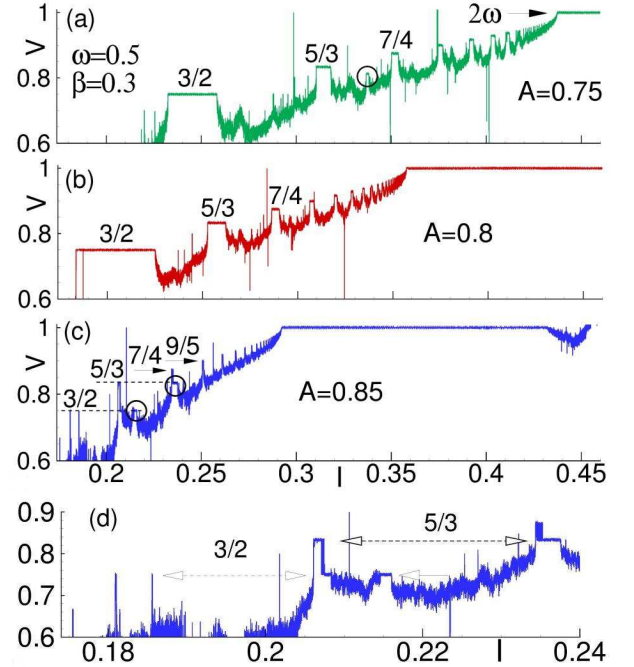


FIG. 7: (Color online)  $A$ -variation of the devil's staircase structure Svetlana at  $\omega = 0.5$ ,  $\beta = 0.3$ . (a)  $A = 0.75$ ; (b)  $A = 0.8$ ; (c)  $A = 0.85$ ; (d) Enlarged part of structure at  $A = 0.85$ , demonstrating overlapping of subharmonics.

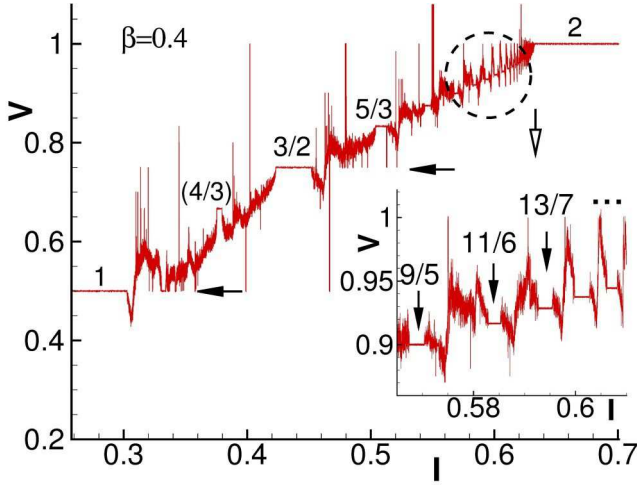


FIG. 8: (Color online) The devil's staircase structure at  $\omega = 0.5$ ,  $A = 0.8$  and  $\beta = 0.4$ . Inset enlarges the part of the structure marked by circle.

The chaotic parts of Svetlana can be essentially modified by changing of JJ parameters. Figure 8 presents the devil's staircase structure in Svetlana at the same radiation parameters  $\omega = 0.5$  and  $A = 0.8$ , but at a different dissipation parameter  $\beta = 0.4$ . We see that the character of chaotic regions is changed, but it still demonstrates regular variation of the steps and chaos. We have also observed here the additional step  $4/3$  (taken in the brackets in figure) which belongs to another continued fraction. The inset enlarges the part of the structure marked by circle. We see clearly the similar character of the chaotic parts for higher steps.

Thus, the answer to the question stated at the beginning of this section is positive: based on our results, we note that the structured chaos is a stable formation over definite intervals of  $A$ . Analogous results are obtained by changing the frequency of radiation  $\omega$ .

## VII. ANALYSIS OF THE EXPERIMENTAL RESULTS

Let us now briefly discuss the existing experimental results. The experimental survey of chaos in the Josephson effect was presented in Ref. [47]. The authors analyzed the range of chaotic behavior in tin tunnel junctions and indium microbridges subjected to dc and rf bias. An important fact found by this detailed analysis was a statement that the experimental results agree with simulations based on the resistively and capacitively shunted junction (RCSJ) model and theoretical predictions. This fact stresses the necessity for further numerical investigations within the RCSJ model.

One of the interesting features of the IV-characteristics under external electromagnetic radiation is a fragmentation of Shapiro steps and their subharmonics. Such frag-

mentation was demonstrated in the numerical results of Kautz and Monako [15]. Experimental evidence of the fragmented IV-characteristics, particularly, strongly distorted steps and "wiggles," which are preceded by subharmonic voltage steps for lower rf powers in Pb/ox/PbIn tunnel junctions and in Pb microbridges irradiated by 70-GHz microwaves were reported in Ref. [54].

The results of the experimental observation of a devil's staircase on a microwave irradiated Josephson junction prepared from the bulk polycrystalline magnetic superconductor  $\text{GdMo}_6\text{Se}_8$  were presented in Ref. [55]. Measurements were made at a temperature of 1.3 K, under external radiation at 9.5 GHz. The authors considered that the possible reason for the appearance of the DS was an overlapping of the steps. We note that the detailed experimental investigation of the fragmented phases at different conditions and parameters of JJ is still lacking. The fragmentation of SS was also observed in our simulations at amplitude  $A < 0.8$ . An increase in amplitude leads to the overlapping of the SS and destroys them. It can be seen in Fig. 1 for SS with  $n < 4$ . Results will be discussed in detail, elsewhere.

Noise rise and negative differential resistance regions in a self-resonant circuit consisting of an inductively and resistively shunted Nb/ox/PbIn tunnel junction were observed by Miracky *et al.* [56]. Gubankov *et al.* [57, 58] investigated the frequency range of chaotic behavior in Nb/ox/PbBi tunnel junctions. Their results are in agreement with the simulations based on RCSJ model.[47] The distorted IV-characteristics and a strong noise rise in the distorted regions, which was ascribed to chaotic noise were found in Ref. [60]. Reports on measurements of dc electron transport and microwave dynamics of thin film hybrid Nb/Au/CaSrCuO/YBaCuO planar Josephson junctions were presented in Ref. [59]. The authors observed tunnel-like behavior, and oscillations in sync with the applied radiation at integer and half-integer steps. For a junction fabricated with a *c*-oriented yttrium barium copper oxide (YBCO) film, the devil's staircase structure was observed under microwave irradiation at 4.26 GHz.

In Refs.[61–63] the authors provide further confirmation for the existence of chaotic regions in the intermediate- and high-McCumber parameter regime. In experiments with short Indium microbridges the devil's staircase transition to chaos was observed. Such data can also be evaluated within the framework of the RCSJ model [47].

Based on the analysis of the experimental investigations of the chaos in the JJ, we note that at present, the experimental observation of structured chaos in the IV-characteristics under external electromagnetic radiation (Svetlana structure) is absent. Since our results on numerical simulations of Svetlana were obtained by the RCSJ model, it would be very interesting to test the formation of the Svetlana structure and its features experimentally.



### VIII. CONCLUSION

We have performed high-precision numerical simulations of the Josephson junction under external microwave radiation, within the well-established RCSJ (Stewart-McCumber) model. Our simulations have indicated the presence of an unusual structure, that occurs within the IV-characteristics of the junction. By analyzing the IV-characteristics, Lyapunov exponents and Poincaré sections we have identified a region of experimentally realizable parameters for which the subharmonic Shapiro steps are separated by structured chaotic windows. We have called this formation, Svetlana.

Interestingly, the dynamics of the system, which follows a deterministic path and exhibits synchronization with the external drive in the form of constant voltage subharmonic steps (Shapiro steps), can be disrupted while a trace of the underlying staircase remains. Since the low rationals in the subharmonic set are more stable and live longer, we obtain a well structured chaos as the steps become interleaved with chaotic windows. There is thus a gradual disappearance of order, as well as resonance overlap. The argument implicitly requires a subharmonic region of the staircase.

An alternative way of looking at this phenomenon is in terms of equivalent lower-dimensional chaotic maps that are interrupted by the ordered dynamics. Such ideas have been conjectured and explored previously [41]. Here we have shown that the multiple devil's staircase property is effectively reproduced by a continuous, differentiable map. We have furthermore identified the diffusive chaotic mode as playing a role similar to the discontinuity in the map [64]. In fact, the diffusive chaos contains an indication of such a discontinuity.

Analysis of the experimental results on chaos in JJ under external radiation have indicated that a whole series of important results obtained by numerical calcu-

lations is still open for experimental investigations. If experimentally confirmed, the results obtained in the present paper could, for example, be applied to topological superconductivity, a field which is currently being investigated intensively [65, 66]. They support Majorana fermions which are expected to be used for realization of quantum gates that are topologically protected from local sources of decoherence. The authors of [67] report the observation of the fractional a.c. Josephson effect in a semiconductor-superconductor nanowire junction as a signature of Majorana quasiparticles. The use of subharmonics for the detection of the Majorana fermions is a very interesting but unsolved problem. Its solution may provide additional information on the Majorana physics and may warrant special consideration in a more detailed investigation.

Finally, we have also demonstrated universality within the diffusively chaotic windows. Such universality is an underlying feature of the chaotic windows; which, while being contained within the staircase itself, are effectively being 'washed' out. We find this aspect of the work most interesting because it shows some sort of predictability, even though we have chaotic dynamics: as if the ghost of the staircase lives on!

### Acknowledgments

Yu. M. S. thanks I. Rahmonov, M. Yu. Kupriyanov, K.Y. Constantinian, G. A. Ovsyannikov, V. P. Koshelets for helpful discussions and D. V. Kamanin and the JINR-SA agreement for the support of this work. He also appreciates kind hospitality of Prof. Y. Takayama and Prof. N. Suzuki from Utsunomiya university where part of this work was done. Yu. M. S. and M. R. K. wish to thank the Physics Department at the University of South Africa for a pleasant stay.

- 
- [1] W. Buckel and R. Kleiner, *Superconductivity: Fundamentals and Applications* (Wiley-VCH, Weinheim, 2004).
  - [2] K. K. Likharev, *Dynamics of Josephson Junctions and Circuits* (Gordon and Breach, Philadelphia, 1986).
  - [3] R. L. Kautz, *Rep. Prog. Phys.* **59**, 935 (1996).
  - [4] Da-Ren He, W. J. Yeh, and Y. H. Kao, *Phys. Rev. B* **31**, 1359 (1985).
  - [5] M. H. Jensen, P. Bak and T. Bohr, *Phys. Rev. Lett.* **50**, 1637 (1983).
  - [6] E. Ben-Jacob, Y. Braiman, R. Shainsky, *Appl. Phys. Lett.* **38**, 822 (1981).
  - [7] V. Nebendahl and W. Dür, *Phys. Rev. B* **87**, 075413 (2013).
  - [8] M. Takigawa et. al., *Phys. Rev. Lett.* **110**, 067210 (2013)
  - [9] H. Weimer and H. P. Büchler, *Phys. Rev. Lett.* **105**, 230403 (2010).
  - [10] R. B. Laughlin et al., *Phys. Rev. B* **32**, 1311 (1985).
  - [11] A. M. Hriscu and Yu. V. Nazarov, *Phys. Rev. Lett.* **110**, 097002 (2013).
  - [12] S. Urazhdin et al., *Phys. Rev. Lett.* **105**, 104101 (2010).
  - [13] B. A. Huberman, J. P. Crutchfield, and N. H. Packard, *Appl. Phys. Lett.* **37**, 750 (1980).
  - [14] R. L. Kautz, *J. Appl. Phys.* **52**, 6241 (1981).
  - [15] R. L. Kautz and R. Monaco, *J. Appl. Phys.* **57**, 875 (1985).
  - [16] R. L. Kautz, *J. Appl. Phys.* **58**, 424 (1985).
  - [17] N. F. Pedersen and A. Davidson, *Appl. Phys. Lett.* **39**, 830 (1981).
  - [18] A. Irie, Y. Kurosu, and G. Oya, *IEEE Trans. Appl. Supercond.* **13**, 908 (2003).
  - [19] J. Scherbel et al., *Phys. Rev. B* **70**, 104507 (2004).
  - [20] T. Bohr, P. Bak, and M. H. Jensen, *Phys. Rev. A* **30**, 1970 (1984).
  - [21] M. H. Jensen, P. Bak, and T. Bohr, *Phys. Rev. A*, **30**, 1960 (1984).
  - [22] P. H. Borchers and G. P. McCauley, *J. Phys. C* **20**, 261 (1987).

- [23] E. Ben-Jacob, Y. Braiman, R. Shainsky, and Y. Imry, Phys. Rev. Lett. **49**, 1599 (1982).
- [24] G. V. Osipov, A. S. Pikovsky and J. Kurths, Phys. Rev. Lett. **88**, 054102 (2002).
- [25] E. Ben-Jacob, Y. Braiman, R. Shainsky, and Y. Imry, Appl. Phys. Lett. **38**, 822 (1981).
- [26] W. J. Yeh and Y. H. Kao, Phys. Rev. Lett. **49**, 1888 (1984).
- [27] H. Seifert, Phys. Lett. A **101**, 230 (1984).
- [28] H. Seifert and C. Noeldeke, in Proceedings of the 17th International Conference on Low Temperature Physics, U. Eckern, A. Schmid, W. Webern, and H. Wühl, eds. (North-Holland, Amsterdam, 1984), p. 1135.
- [29] C. Noeldeke and H. Seifert, Phys. Lett. A **109**, 401 (1985).
- [30] H. Seifert, Phys. Lett. A **98**, 213 (1983).
- [31] P. Manneville and Y. Pomeau, Phys. Lett. A **75**, 1 (1979).
- [32] Y. Pomeau and P. Manneville, Commun. Math. Phys. **51**, 231 (1984).
- [33] Y. Pomeau and P. Manneville, Commun. Math. Phys. **74**, 189 (1980).
- [34] Sebastien Petit-Watlot *et al.*, Nature Physics **8**, 682 (2012).
- [35] T. P. Valkering, C. L. A. Hooijer, and M. F. Kroon, Physica D **135**, 137 (2000).
- [36] Sadataka Furui and Tomoyuki Takano, arXiv:1312.3001v2 [nlin.CD] 25Jan2014.
- [37] P. Reimann *et al.*, Phys. Rev. E **65**, 031104 (2002).
- [38] David Speer, Ralf Eichhorn, and Peter Reimann, Phys. Rev. E **76**, 051110 (2007).
- [39] A. Macor, F. Doveil, and Y. Elskens, Phys. Rev. Lett. **95**, 264102 (2005).
- [40] Yu. M. Shukrinov, S. Yu. Medvedeva, A. E. Botha, M. R. Kolahchi, and A. Irie, Phys. Rev. B **88**, 214515 (2013).
- [41] Shi-Xian Qu, Shunguang Wu, and Da-Ren He, Phys. Rev. E **57**, 402 (1998).
- [42] W. C. Stewart, Appl. Phys. Lett. **12**, 277 (1968).
- [43] D. E. McCumber, J. Appl. Phys. **39**, 3113 (1968).
- [44] Yu. M. Shukrinov and M. A. Gaafar, Phys. Rev. B **84**, 094514 (2011).
- [45] Yu. M. Shukrinov, M. Hamdipour, M. R. Kolahchi, A. E. Botha, and M. Suzuki, Phys. Lett. A **376**, 3609 (2012).
- [46] This is the first name of the third author, who first found it in her numerical simulations.
- [47] C. Noeldeke, R. Gross, M. Bauer, G. Reiner, and H. Seifert, Journal of Low Temperature Physics **64**, 225 (1986).
- [48] R. C. Hilborn, Chaos and Nonlinear Dynamics: An Introduction (Oxford University Press, New York, 2000), 2nd edition.
- [49] P. Bak, Physics Today **39**, 38 (1986).
- [50] M. J. Feigenbaum, J. Stat. Phys. **21**, 669 (1979).
- [51] M. J. Feigenbaum, Los Alamos Science **1**, 4 (1980).
- [52] M. Gitterman, The Chaotic Pendulum (World Scientific, Singapore, 2010).
- [53] Antonio Barone and Gianfranco Paterno Physics and Applications of the Josephson Effect (John Wiley and Sons, New York, 1982).
- [54] K. Okuyama, H. J. Hartfuss, and K. H. Gundlach, J. Low Temp. Phys. **44**, 283 (1981).
- [55] J. Kuznik and K. Rogacki, Physics Letters A **176**, 144 (1993).
- [56] R. F. Miracky, J. Clarke, and R. H. Koch, Phys. Rev. Lett. **50**, 856 (1983).
- [57] V. N. Gubankov, K. I. Konstantinyan, V. P. Koshelets, and G. A. Ovsyannikov, IEEE Trans. Magn. **19**, 637 (1983).
- [58] V. N. Gubankov, S. L. Ziglin, K. I. Konstantinyan, V. P. Koshelets, and G. A. Ovsyannikov, Zh. Eksp. Tear. Fiz. **86**, 3453 (1984) [Soy. Phys. JETP **59**, 198 (1984)].
- [59] K. Y. Constantinian *et al.*, JPCS **234**, 042004 (2010).
- [60] M. Octavio and C. R. Nasser, Phys. Rev. B **30**, 1586 (1984).
- [61] C. Vanneste, C. C. Chi, and D. C. Cronmeyer, Phys. Rev. B **32**, 4796 (1985).
- [62] M. Iansiti, Qing-Hu, R. M. Westerfield, and M. Tinkham, Phys. Rev. Lett. **55**, 746 (1985).
- [63] D.C. Cronmeyer, C. C. Chi, A. Davidson, and N. F. Pedersen, Phys. Rev. B **31**, 2667 (1985).
- [64] M. Bauer, S. Habip, D. R. He, and W. Martienssen, Phys. Rev. Lett. **68**, 1625 (1992).
- [65] R. M. Lutchyn, J. D. Sau, S. D. Sarma, Phys. Rev. Lett. **105**, 077001 (2010).
- [66] J. Alicea, Y. Oreg, G. Refael, F. von Oppen, M. P. A. Fisher, Nature Physics. **7**, 412 (2011).
- [67] Leonid P. Rokhinson, Xinyu Liu and Jacek K. Furdyna, Nature Physics **8**, 795 (2012).